

## Video Article

# Impacts of Free-falling Spheres on a Deep Liquid Pool with Altered Fluid and Impactor Surface Conditions

Daren A. Watson<sup>1</sup>, Jeremy L. Stephen<sup>1</sup>, Andrew K. Dickerson<sup>1</sup><sup>1</sup>Department of Mechanical and Aerospace Engineering, University of Central FloridaCorrespondence to: Andrew K. Dickerson at [dickerson@ucf.edu](mailto:dickerson@ucf.edu)URL: <https://www.jove.com/video/59300>DOI: [doi:10.3791/59300](https://doi.org/10.3791/59300)

Keywords: Engineering, Issue 144, engineering, cavity formation, fluid dynamics, hydrophilic, hydrophobic, protocol, splashing, water entry, wetting, Worthington jet

Date Published: 2/17/2019

Citation: Watson, D.A., Stephen, J.L., Dickerson, A.K. Impacts of Free-falling Spheres on a Deep Liquid Pool with Altered Fluid and Impactor Surface Conditions. *J. Vis. Exp.* (144), e59300, doi:10.3791/59300 (2019).

## Abstract

Vertical impacts of spheres on clean water have been the subject of numerous water entry investigations characterizing cavity formation, splash crown ascension and Worthington jet stability. Here, we establish experimental protocols for examining splash dynamics when smooth free-falling spheres of varying wettability, mass, and diameter impact the free surface of a deep liquid pool modified by thin penetrable fabrics and liquid surfactants. Water entry investigations provide accessible, easily assembled and executed experiments for studying complex fluid mechanics. We present herein a tunable protocol for characterizing splash height, flow separation metrics, and impactor kinematics, and representative results which might be acquired if reproducing our approach. The methods are applicable when characteristic splash dimensions remain below approximately 0.5 m. However, this protocol may be adapted for greater impactor release heights and impact velocities, which augurs well for translating results to naval and industry applications.

## Video Link

The video component of this article can be found at <https://www.jove.com/video/59300/>

## Introduction

The characterization of splash dynamics arising from vertical impacts of solid objects on a deep liquid pool<sup>1</sup> is applicable to military, naval and industrial applications such as ballistic missile water entry and sea surface landing<sup>2,3,4,5</sup>. The first studies of water entry were conducted well more than a century ago<sup>6,7</sup>. Here, we establish clear in-depth protocols and best practices for achieving consistent results for water entry investigations. To aid valid experimental design, a method is presented for the maintenance of sanitary conditions, alteration of interfacial conditions, control of dimensionless parameters, chemical modification of impactor surface, and visualization of splash kinematics.

Vertical impacts of free-falling hydrophilic spheres on the quiescent fluid show no sign of air-entrapment at low velocities<sup>8</sup>. We find that the placement of thin penetrable fabrics atop the fluid surface causes cavity formation due to forced flow separation<sup>1</sup>. A meager amount of fabric on the surface amplifies splashing across a range of moderate Weber numbers while sufficient layering attenuates splashing as spheres overcome drag at fluid entry<sup>1</sup>. In this article, we explain protocols suitable for establishing the effects of material strength on the water entry of hydrophilic spheres.

Cavity forming splashes from hydrophobic impactors show the ascension of a well-developed splash crown, followed by the protrusion of the primary jet high above the surface when compared to their water-liking counterparts<sup>8</sup>. Here, we present an approach for achieving water repellency through chemically modifying the surface of hydrophilic spheres.

With the advent of high-speed cameras, splash visualization and characterization have become more attainable. Even so, established standards in the field call for the use of a single camera orthogonal to the primary axis of travel. We show that the use of an additional high-speed camera for overhead views is necessary to adjudge spheres strike the intended location.

## Protocol

### 1. Configuring the experiment for vertical impacts

1. Fill a transparent water tank of dimensions approximately 60 cm x 30 cm x 36 cm (length x width x depth) with 32 L of water and mount a meter ruler ('visual scale') vertically inside the container such that the base sits atop the fluid, as seen in **Figure 1a**.  
NOTE: Depth and width of the tank must be greater than 20 times the diameter of the largest spheres used in the experiment to ensure wall effects are negligible<sup>9</sup>. Greater entry speeds than those described here will require greater tank depth. The visual scale used to determine drop heights and calibration of tracking software is discussed in section 7.

2. Place an additional meter ruler under the water, which can act to magnify dimensions. This visual scale is used for calibrating tracking software for underwater measurements.
3. Construct a hinged platform ('release mechanism') that suspends spheres above the fluid and rotates downward, to achieve tangential acceleration greater than gravity at the impactor location when released, as seen in **Figure 1a**. Rapid rotation is achieved by connecting the hinged platform to the center of the supporting component using elastic bands. The result is an unsupported and non-rotating impactor.  
NOTE: The platform is easily fabricated with 3D printer.
4. For impact trials, place thumb to base of hinged platform and rotate it 90° to a horizontal position for placement of spheres above the fluid.  
NOTE: Retraction is triggered when thumb is released from base of the platform.
5. Affix the release mechanism to a retort stand, such that the device can be adjusted to various heights.
6. Place the retort stand next to the tank such that the release mechanism is within the same depth plane as the visual scale. Add a weight to the base of the retort stand as needed to prevent toppling.
7. Adjust the release mechanism to the maximum desired experimental drop height. This is necessary for optimal splash visualization as discussed in section 6 and ensures the splash characteristics of interest are always within the viewing frame of the camera.
8. Attach a multi-LED light to an articulating arm such that the light is mounted above the camera, looking down onto the splash zone. Ambient light alone is insufficient to illuminate the scene at the high frame rates needed to extract splash kinematics.  
NOTE: One can never have too much light.
9. Place a black screen at the back of the water tank to aid splash and cavity visualization as seen in **Figure 2**.
10. Place a glass-protecting shock absorber, such as a closed-cell sponge, at the bottom of water tank and affix with weights to prevent resurfacing.  
NOTE: The height of the fluid in the tank should be such that the sphere does not interact with shock absorber prior to air cavity pinch off<sup>10</sup>.

## 2. Controlling dimensionless parameters

1. Conduct experiments with smooth spheres of various masses and diameters. For this, polyoxymethylene (e.g., Delrin) coin-making balls work particularly well and have no mold part line. Measure masses and diameters with an analytical balance and Vernier caliper respectively.
2. Conduct experiments over a range of heights  $H$  to generate impact velocities  $U \approx \sqrt{2 \cdot g \cdot H}$  where  $g = 9.81 \text{ m/s}^2$  is the acceleration due to gravity. Measure height with the visual scale within the camera frame.  
NOTE: Use the **Auto-Tracking** feature in the video analysis tool as discussed in section 7 to measure impact velocities.
3. Conduct experiments with fluid mixtures of water and suitable surfactants (e.g., glycerin or soap) to modify surface tension. Measure surface tension with a surface tensiometer.
4. Calculate Reynolds numbers  $Re = \rho \cdot U \cdot D / \mu$  and Weber numbers  $We = \rho \cdot U^2 \cdot D / \sigma$ , where  $\rho$  is the density of the fluid,  $D$  is the sphere diameter,  $\mu$  is the dynamic viscosity of the fluid and  $\sigma$  the surface tension of the fluid.

## 3. Maintaining sanitary experimental conditions

1. Conduct experiments while wearing industrial nitrile gloves and retrieve spheres from water tank with a sanitized scoop.  
CAUTION: Skin naturally produces oils which can affect the wettability of impactors and taint fluid conditions.
2. Clean the spheres with 99% isopropyl alcohol and allow to dry for 1 min in between trials to preclude the influence of impurities.
3. If using fabrics that break apart during impact, replace the water in the tank after every trial if scraps cannot be manually collected.
4. At the end of experiment, empty the tank and leave it to dry.
5. Before an experiment, clean the tank with water to remove any impurities.

## 4. Layering the surface with penetrable fabrics

1. Separate the fabric into square or round plies in preparation for impact trials. Use a Vernier caliper to obtain compressed thickness of the fabric.  
NOTE: Fabric thickness will change when wet.
2. Gently rest the dry fabric atop the surface of the liquid pool. Ensure that the plies do not begin descent before impactor release and replace fabrics immediately after collision.
3. Use a sanitized scoop to position the fabric below the hinged platform before releasing spheres.
4. (Optional) Conduct the following tests using a fabric sample for material characterization.
  1. Perform **tensile testing** using a tensile tester to determine the elastic modulus of the sample.
  2. Use a digital microscope to obtain a microscopic view of the fabric and determine **fiber length** using an imaging tool.

## 5. Preparing chemically hydrophobic spheres

1. Spray the hydrophobic base coat approximately 15–30 cm from the sphere surface. Avoid soaking the surface. Let it dry for 1–2 min before adding additional coatings. Apply two more base coats. Allow it to dry for 30 min before applying the top coat.  
NOTE: The number of additional surface may vary based on recommendations from the product manufacturer.
2. Spray the hydrophobic top coat approximately 15–30 cm from the surface. Avoid soaking the surface. Let it dry for 1–2 min before adding additional coatings. Apply two or three more coatings of top coat. Allow to dry for 30 min for light use and 12 h for full use.  
NOTE: The number of additional surface coats may vary based on recommendations from the product manufacturer.
3. After approximately 20 trials, the hydrophobic coating becomes compromised due to excessive handling. Remove coating with 99% isopropyl and repeat steps 5.1 and 5.2.

## 6. Synchronizing cameras for splash visualization

1. Place a high-speed camera with a suitable lens perpendicular to the impact axis and in-line with the surface of the fluid.  
NOTE: A 55 mm prime lens provides a good starting point.
2. Where fabrics are to be used, add an additional high-speed camera to the experiment to provide a top-down view of the impacts, as seen in **Figure 1b**.
3. Synchronize multiple cameras to a computer using the following steps.
  1. Connect both output terminals of the horizontal camera to both input terminals of the additional camera using BNC cables.
  2. Connect the trigger switch to the horizontal camera only.
  3. Plug Ethernet cables from both cameras into an off-network router connected to the computer.  
NOTE: In the absence of a router, connect Ethernet cables of cameras to separate computers.
4. In the video acquisition software, configure the cameras with the following settings. Set frame rate to a minimum of 1,000 fps, set screen resolution to the desired resolution. Set the shutter speed to 1 per frame second and set trigger mode to end.
5. From maximum release height, conduct a series of test trials to ensure that the Worthington jets are within the video frame.
6. Adjust the camera position and focus accordingly until the desired visualization quality is achieved.
7. After recording, extract kinematic and geometric measurements from videos using a suitable video analysis tool. Use **Tracker**, an open source analysis tool or any software of comparative capability.

## 7. Digitizing impact kinematics with tracker software

1. Select **calibration stick** from the Tracker toolbox and match it to the visual scale (**Figure 2a**), making the stick as long as possible.
2. Click **calibration stick** and set the scaling value to the length of the visual scale spanned by the stick. That is, if the calibration stick spans 1 cm on visual scale, set scaling value to 1.  
NOTE: This ensures measurements taken from software are in the order of centimeters.
3. Toggle video playback by clicking **start** and **stop** and set video to the desired frame.
4. Select **measuring stick** from the Tracker toolbox and extract splash crown height  $k$ , cavity width  $b$ , cavity depth  $l$ , and Worthington jet height  $h$ , as seen in **Figure 2b,c**.  
NOTE: The measuring stick is adjustable at both ends and can be used simultaneously with other toolbox selections.
5. Select **protractor** from the Tracker toolbox and measure the separation angle  $q$  of fluid with respect to the impactor, as seen in **Figure 2b**. The protractor is adjustable at both ends and can be used simultaneously with other toolbox selections.
6. Select the **Auto-Tracking** feature in the software to record temporal position and velocity data. When tracking is interrupted due to lack of clarity in the video, use manual tracking until clarity is obtained and auto-tracking is resumed.

## Representative Results

This established protocols allow for the observance of the Worthington jets arising from vertical impacts over a range of Weber numbers  $We$  as seen in **Figure 2c**. These results are published in Watson et al.<sup>1</sup>, which can be referenced for the exact experimental conditions used to produce the data presented herein. We focus on the narrow elongated film of fluid protruding above the free liquid surface. In **Figure 3** we show a meager amount of fabric amplifies splashing while sufficient layering attenuates splash back. Results are non-dimensionalized using the sphere diameter  $D$  as seen in **Figure 3b**.

We show the relation between non-dimensionalized cavity properties such as cavity depth  $\lambda^*$ , splash crown height  $\kappa^*$ , cavity width  $\beta^*$  and Weber number  $We$  in **Figure 4a-d**. Results are captured with a single frontal high-speed camera in a well-lit environment. A representative camera view is seen in **Figure 2b**. Across the range of experimental  $We$  in **Figure 4**, dimensions of cavities created by a sphere impacting a single layer of fabric show little variation.

We consider the trajectory of spheres after impact with the interfacial surface and track temporal position data until cavity pinch off occurs as seen in **Figure 5a**. We then smooth the data with a Savitzky-Golay filter<sup>11</sup> to remove the effects of experimental noise prior to numerical differentiation. The resulting velocity curves in **Figure 5b** are again smoothed prior to numerical differentiation for obtaining  $du/dt$  necessary for force analysis.

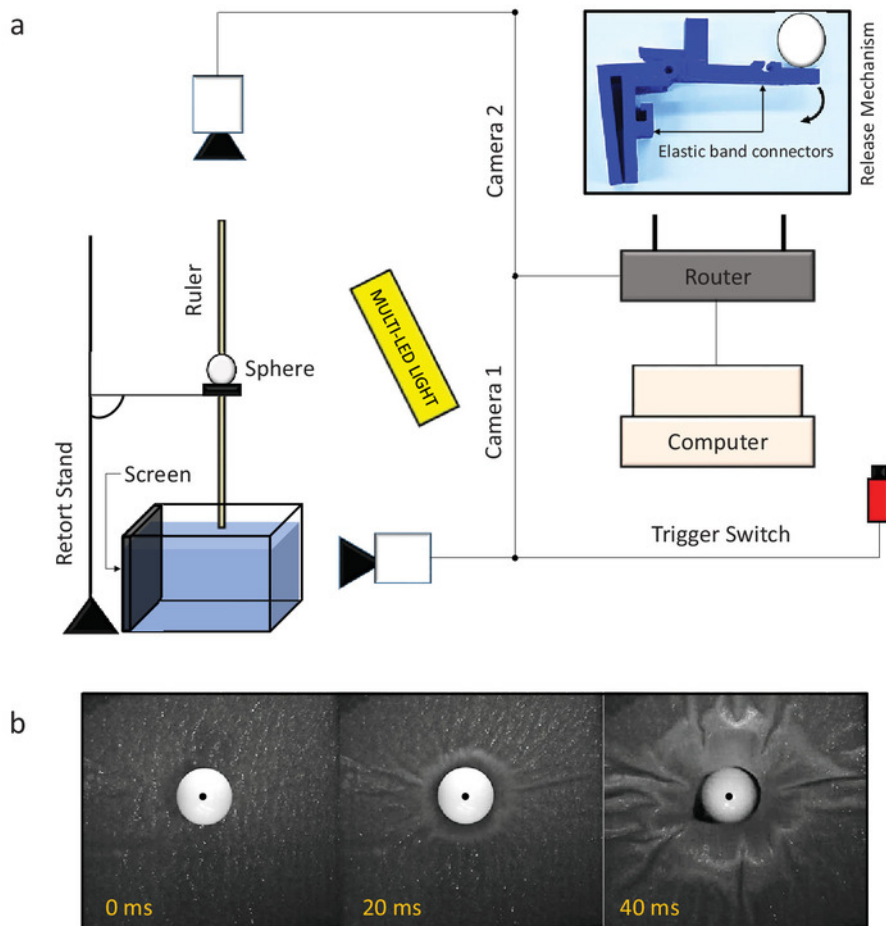


**Figure 1. Schematic of the experimental setup.** (a) High-speed cameras capture frontal and overhead views with diffuse lighting positioned above the frontal camera. The trigger switch is optional, given the availability of manual controls in video recording software on the computer. (b) Photo sequence of hydrophilic sphere impact on a thin penetrable fabric atop the fluid, filmed using the overhead camera. A black dot is used to ensure no rotation present during free fall. [Please click here to view a larger version of this figure.](#)

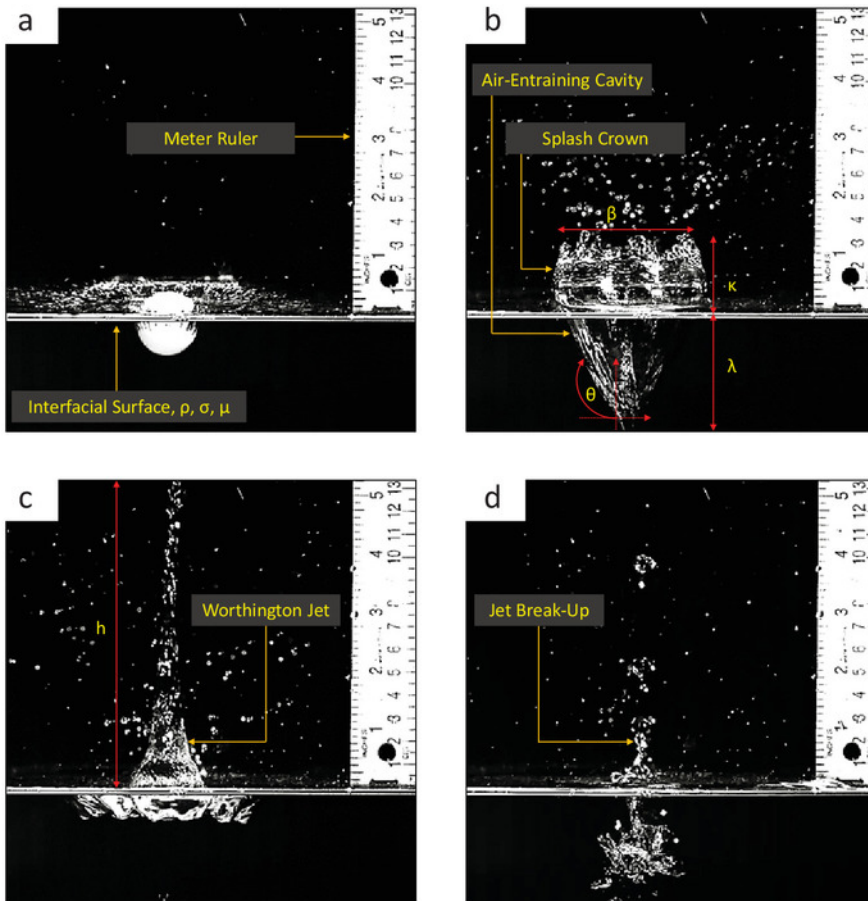


**Figure 2. Splash visualization for hydrophobic sphere impact on an unaltered surface.** The photo sequence shows (a) water entry, (b) splash crown ascension and air-entrapment, (c) Worthington jet formation and, (d) jet breakup for a representative splash. Sphere has impact velocity of  $U = 3.5$  m/s. A meter stick is used to calibrate measurements within the video analysis tool, used to measure splash crown height  $\kappa$ , cavity width  $\beta$ , cavity depth  $\lambda$ , separation angle  $\theta$  and Worthington jet height  $h$ . [Please click here to view a larger version of this figure.](#)

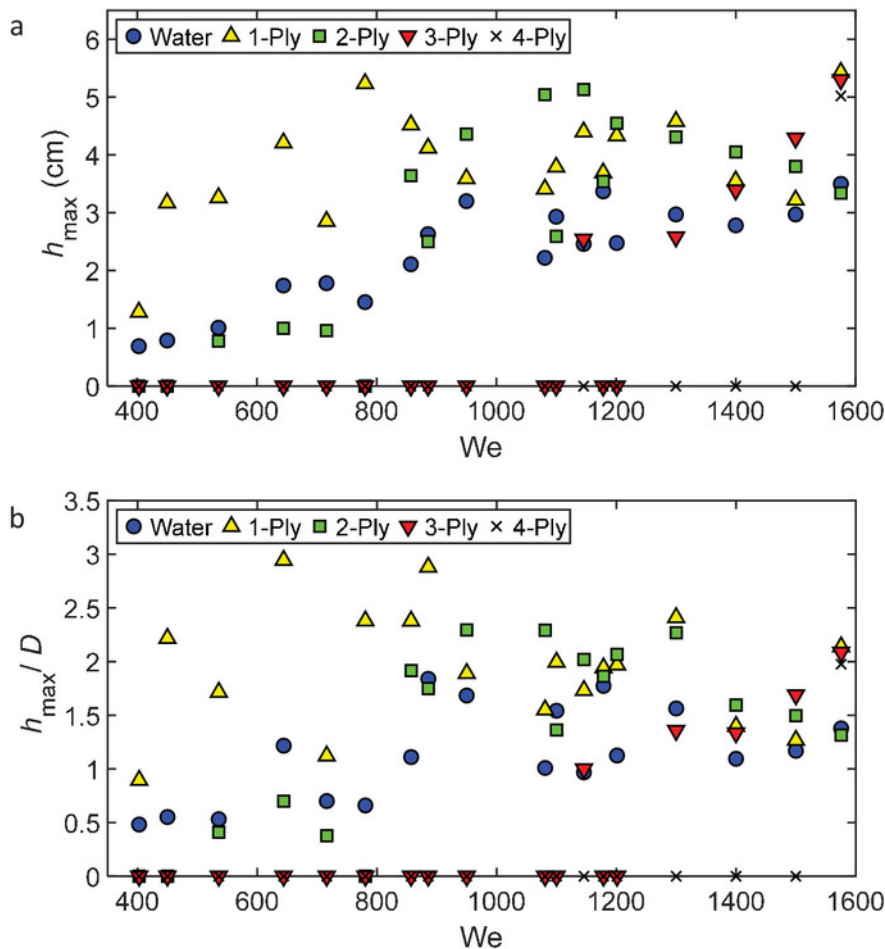


**Figure 3. Splash heights across Weber number ( $We$ ).** (a) Worthington jet height  $h_{max}$  vs.  $We$ , with  $h_{max}/D$  vs.  $We$  shown in (b). Number preceding "Ply" denotes the layers of fabric. [Please click here to view a larger version of this figure.](#)

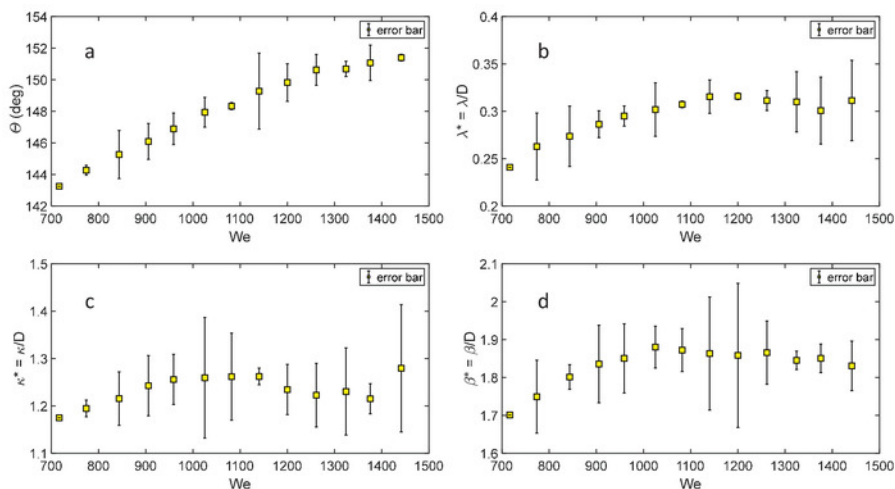


**Figure 4. Variation of cavity dimensions across Weber numbers.** Relation between  $We$  and the (a) separation angle  $\theta$ , (b) cavity depth  $\lambda$ , (c) splash crown height  $\kappa$ , and (d) cavity width  $\beta$ . Properties are non-dimensionalized in terms of sphere diameter,  $D$ . Error bars denote standard deviation for the average of five trials at each point. Figure is modified from Watson et al.<sup>1</sup>. [Please click here to view a larger version of this figure.](#)

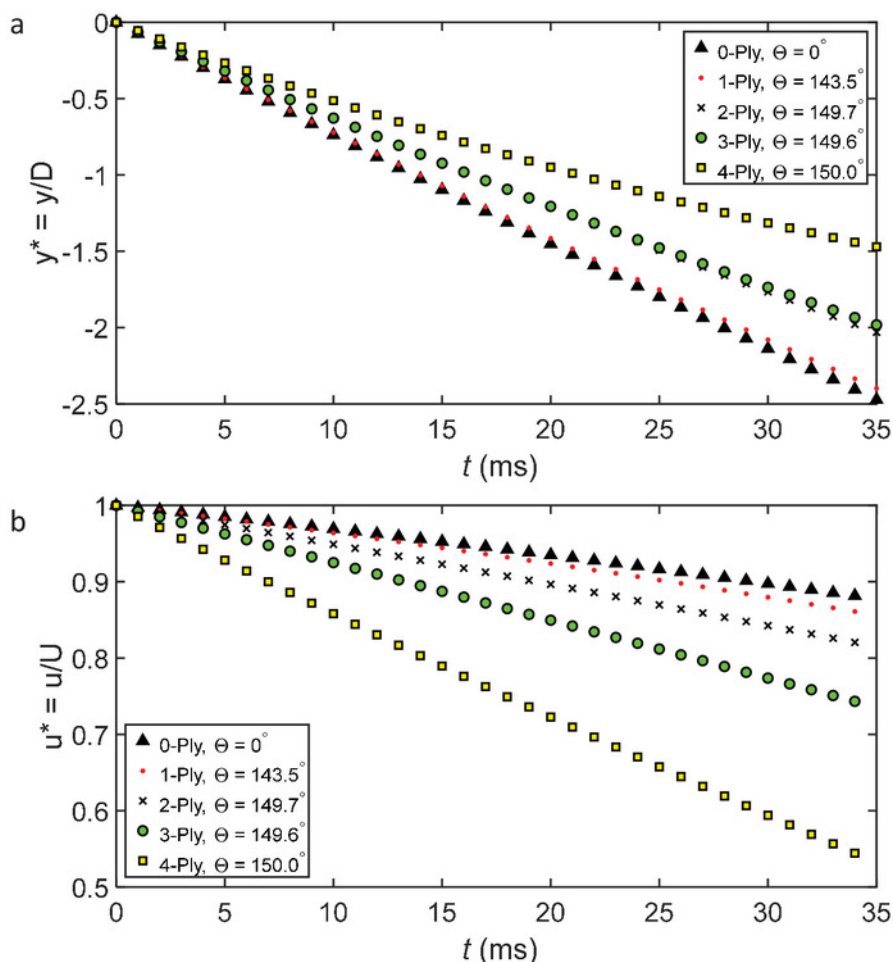


**Figure 5. Representative kinematics of sphere during underwater descent.** Temporal tracks of (a) vertical position  $y$  and (b) velocity  $u$  for impacting spheres with 0- to 4- layers of fabric atop the water. Trajectories are non-dimensionalized in terms of the sphere diameter,  $D$  and impact velocity  $U$  respectively. [Please click here to view a larger version of this figure.](#)

## Discussion

This protocol describes the experimental design and best practices for investigations of free-falling spheres onto a deep liquid pool. We begin by highlighting steps necessary for configuring the experiment for vertical impacts. It is important to create an ideal splash environment with the use of a sufficiently large splash zone such that wall effects are negligible<sup>9</sup>, and a suitable visual scale for extracting kinematics<sup>12,13,14,15,16,17,18,19,20,21</sup>. While shock absorbers can be improvised from excess lab materials, they must be sanitized before the experiment with water and a suitable dirt removing agent. Failure to clean the shock absorber and the tank can lead to the introduction of impurities during an experiment and alter splash characteristics. In the literature, there exists a lack of detail regarding maintenance of experimental cleanliness and as such, this article presents guidelines for obtaining consistent results from water entry trials.

The techniques described above are subject to tuning as seen in previous studies. The spring-actuated release mechanism employed by the authors can be substituted with electromagnets<sup>15</sup> when using ferrous spheres. The ease of use of the method is improved when high-speed cameras are set to automatically trigger after spheres fall through photocells<sup>12</sup> or infrared triggers<sup>22,23</sup>, but these add complexity. Impactor surface treatments to control wettability can also be done by using more rigorous approaches as seen in Duez et al.<sup>8</sup>. For example, spheres grafted with octyltriethoxysilane, rinsed with isopropyl and heated in an oven at  $90^\circ\text{C}$  achieve super-hydrophobicity<sup>8</sup>. The protocol can be further tuned for improved cavity visualization by replacing the black screen (shown in **Figure 1a**) with backlighting, which makes cavity features more pronounced<sup>3</sup>.

Care should be taken when considering temporal kinematics for theoretical investigations. Temporal position tracks present less distortion than for velocity tracks but require smoothing prior to numerical differentiation<sup>1,3,15</sup>. The Savitzky-Golay filter performs a polynomial regression on a range of equally spaced values to determine the smoothed value for each point and can more faithfully maintain a track's salient features<sup>11</sup>. For tracking sphere position, a second-degree polynomial within the Savitzky-Golay filter preserves the track's salient features while removing experimental noise. Finally, researchers have choice of the moving average span of the filter, which should be as small as possible while still achieving the desired level of smoothing.

The established protocol is not restricted to the list of materials presented here and can be undertaken on a larger scale to generate greater impact velocities and increased range of dimensionless parameters which augurs well for translating results to naval and industry applications.

## Disclosures

The authors have nothing to disclose.

## Acknowledgments

The authors would like to acknowledge the College of Engineering and Computer Sciences (CECS) at the University of Central Florida for funding this project, Joshua Bom and Chris Souchik for splash imagery and Nicholas Smith for valuable feedback.

## References

1. Watson, D. A., Stephen, J. L., Dickerson, A. K. Jet amplification and cavity formation induced by penetrable fabrics in hydrophilic sphere entry. *Physics of Fluids*. **30**, 082109 (2018).
2. Truscott, T. T. *Cavity dynamics of water entry for spheres and ballistic projectiles*. Doctor of Philosophy Thesis, Massachusetts Institute of Technology. (2009).
3. Truscott, T., Techet, A. Water entry of spinning spheres. *Journal of Fluid Mechanics*. **625**, 135 – 165 (2009).
4. Techet, A., & Truscott, T. Water entry of spinning hydrophobic and hydrophilic spheres. *Journal of Fluids and Structures*. 716 (2011).
5. Zhao, S., Wei, C., Cong, W. Numerical investigation of water entry of half hydrophilic and half hydrophobic spheres. *Mathematical Problems in Engineering*. **2016**, 1–15 (2016).
6. Worthington, A. M., Cole, R. S. Impact with a liquid surface studied by the aid of instantaneous photography. *Philosophical Transactions of the Royal Society of London*. 137 (1897).
7. Worthington, A. M., Cole, R. S. Impact with a liquid surface studied by the aid of instantaneous photography. Paper II. *Philosophical Transactions of the Royal Society of London*. 175 (1900).
8. Duez, C., Ybert, C., Clanet, C., & Bocquet, L. Making a splash with water repellency. *Nature Physics*. **3**, 180 – 183 (2007).
9. Tan, B. C. W., Thomas, P. J. Influence of an upper layer liquid on the phenomena and cavity formation associated with the entry of solid spheres into a stratified two-layer system of immiscible liquids. *Physics of Fluids*. **30**, 064104 (2018).
10. Shin, J., McMahon, T. A. The tuning of a splash. *Physics of Fluids*. **2**, 1312–1317 (1990).
11. Krishnan, S. R., Seelamantula, C. S. 2013 On the selection of optimum Savitzky-Golay filters. *IEEE Transactions on Signal Processing*. **61**, 380–391 (2013).
12. Cheny, J., Walters, K. Extravagant viscoelastic effects in the Worthington jet experiment. *Journal of Non-Newtonian Fluid Mechanics*. **67**, 125 – 135 (1996).
13. Castillo-Orozco, E., Davanlou, A., K. Choudhury, P., Kumar, R. Droplet impact on deep liquid pools: Rayleigh jet to formation of secondary droplets. *Physical Review E*. **92**, (2015).
14. Aristoff, J. M., Truscott, T. T., Techet, A. H., Bush, J. W. M. The water entry cavity formed by low bond number impacts. *Physics of Fluids*. **20**, 091111 (2008).
15. Aristoff, J., Bush, J. Water entry of small hydrophobic spheres. *Journal of Fluid Mechanics*. **619**, 45 – 78 (2009).
16. Aristoff, J., Truscott, T., Techet, A., & Bush, J. The water entry of decelerating spheres. *Physics of Fluids*. **22**, (2010).
17. Truscott, T., Epps, B., Techet, A. Unsteady forces on spheres during free-surface water entry. *Journal of Fluid Mechanics*. **704**, 173 – 210 (2012).
18. Truscott, T. T., Epps, B. P., Belden, J. Water entry of projectiles. *Annual Review of Fluid Mechanics*. **46**, 355 – 378 (2013).
19. Gekle, S., Gordillo, J. M. Generation and breakup of Worthington jets after cavity collapse part 1. *Journal of Fluid Mechanics*. **663**, 293–330 (2010).
20. Cross, R., Lindsey, C. Measuring the drag force on a falling ball. *The Physics Teacher*. 169 (2014).
21. Cross, R. Vertical impact of a sphere falling into water. *The Physics Teacher*. 153 (2016).
22. Dickerson, A. K., Shankles, P., Madhavan, N., Hu, D. L. Mosquitoes survive raindrop collisions by virtue of their low mass. *Proceedings of the National Academy of Sciences*. **109** (25), 9822–9827, (2012).
23. Dickerson, A. K., Shankles, P., Hu, D. L. Raindrops push and splash flying insects. *Physics of Fluids*. **26**, 02710, (2014).